Magnetic Resonance Imaging 53 (2018) 52–62

Contents lists available at ScienceDirect

Magnetic Resonance Imaging

journal homepage: www.elsevier.com/locate/mri

Original contribution

4D flow MRI for the analysis of celiac trunk and mesenteric artery stenoses

Florian Siedek[a,*], Daniel Giese[a], Kilian Weiss[a,c], Sandra Ekdawi[a], Sebastian Brinkmann[b], Wolfgang Schroeder[b], Christiane Bruns[b], De-Hua Chang[a], Thorsten Persigehl[a], David Maintz[a], Stefan Haneder[a]

[a] Institute of Diagnostic and Interventional Radiology, University of Cologne, Kerpener Str. 62, 50937 Cologne, Germany
[b] Department of General, Visceral and Tumor Surgery, University of Cologne, Kerpener Str. 62, 50937 Cologne, Germany
[c] Philips Healthcare Germany, Hamburg, Germany

ARTICLE INFO

Keywords:
4D flow MRI
Celiac artery
Superior mesenteric artery
Vessel stenosis
Blood flow characteristics

ABSTRACT

Purpose: This study aims to assess the feasibility of 4D flow MRI measurements in complex vascular territories; namely, the celiac artery (CA) and superior mesenteric artery (SMA).

Materials and methods: In this prospective study, 22 healthy volunteers and 10 patients were scanned at 3 T. Blood flow parameters were compared between healthy volunteers and patients with stenosis of the CA and/or SMA as a function of stenosis grade characterized by prior contrast-enhanced computed tomography (CE-CT). The 4D flow MRI acquisition covered the CA, SMA and adjusting parts of the abdominal aorta (AO). Measurements of velocity- (peak velocity [PV], average velocity [AV]) and volume-related parameters (peak flow [PF], stroke volume [SV]) were conducted. Further, stenosis grade and wall shear stress in the CA, SMA and AO were evaluated.

Results: In patients, prior evaluation by CE-CT revealed 11 low- and 5 mid-grade stenoses of the CA and/or SMA. PV and AV were significantly higher in patients than in healthy volunteers [PV: $p < 0.0001$; AV: $p = 0.03$, $p < 0.001$]. PF and SV did not differ significantly between healthy volunteers and patients; however, a trend towards lower PF and SV could be detected in patients with mid-grade stenoses. Comparison of 4D flow MRI with CE-CT revealed a strong positive correlation in estimated degree of stenosis (CA: $r = 0.86$, SMA: $r = 0.98$). Patients with mid-grade stenoses had a significantly higher average WSS magnitude (AWM) than healthy volunteers ($p = 0.02$).

Conclusion: This feasibility study suggests that 4D flow MRI is a viable technique for the evaluation of complex flow characteristics in small vessels such as the CA and SMA. 4D flow MRI approves comparable to the morphologic assessment of complex vascular territories using CE-CT but, in addition, offers the functional evaluation of flow parameters that goes beyond the morphology.

1. Introduction

The non-invasive evaluation of flow parameters for the characterization and quantification of blood flow in blood vessels is clinically well-established. Such flow characteristics have been determined using color-coded duplex ultrasonography or time-resolved two-dimensional (2D), phase-contrast magnetic resonance imaging (PC-MRI) [1]. However, color-coded duplex ultrasonography can be extremely challenging in some vessel territories due to a restricted acoustic window, while 2D PC-MRI is hampered by several intrinsic technical drawbacks such as the need for accurate planning in order to obtain the necessary perpendicular orientation to the vessel.

Already in the mid 1990s, a further development of 2D PC-MRI was introduced, adding a third spatial dimension to the technique, and resulting in a time-resolved, three-dimensional (3D) PC-MRI acquisition, often referred to as 4D flow MRI [2, 3]. The development of new acceleration techniques exploiting spatio or spatio-temporal correlations of the data made 4D flow feasible in acceptable scan times [4–8]. It is increasingly used for scientific purposes and continues to gain importance in complex clinical cases [9]. With this technical approach, blood or CSF flow can be measured in a user-selected 3D volume [10–12]. 4D flow MRI allows the retrospective, time-resolved, three-

Abbreviations: CA, celiac artery; SMA, superior mesenteric artery; AO, Aorta abdominalis; PV, peak velocity [cm/s]; AV, average velocity [cm/s]; PF, peak flow [ml/s]; SV, stroke volume [ml/hb (heartbeat)]; AWM, average wall shear stress magnitude (N/m^2); CE-CT, contrast-enhanced computed tomography; HV, healthy volunteer; LG, patients with low-grade stenosis of the CA and/or SMA; MG, patients with middle-grade stenosis of the CA and/or SMA

* Corresponding author at: University Hospital of Cologne, Kerpener Str. 62, 50937 Cologne, Germany.
E-mail address: florian.siedek@uk-koeln.de (F. Siedek).

https://doi.org/10.1016/j.mri.2018.06.021
Received 24 March 2018; Received in revised form 31 May 2018; Accepted 28 June 2018

dimensional visualization and evaluation of the vessel territory.

Possible analyses comprise flow parameters such as flow velocity or flow volume in arbitrary spatial planes and slices within the acquired volume [10].

Some more advanced, technically elusive parameters such as the wall shear stress are still under investigation, but first promising results have been reported [13]. The apparent advantages of 4D flow MRI compared to 2D PC-MRI lie in the significant potential for clinical applications for which the evaluation of a bigger proportion of a vessel or the heart is substantial compared to just one slice (e.g. stenosis evaluation; aneurysm evaluation; complex heart diseases). Fortunately, appropriate acquisition sequences and post-processing tools became commercially available. Moreover, an important consideration given the severity of nephrogenic systemic fibrosis is that the administration of contrast agents is not necessary for 4D flow MRI compared to 3D contrast-enhanced MR angiography.

Several current studies have broadened the understanding of pathophysiological mechanisms leading to changes in hemodynamics in different diseases through analyses of complex flow patterns using 4D flow MRI [14, 15]. In these publications, pathologies were associated with aberrant flow characteristics which were challenging or impossible to detect and understand using the current clinical standard. To date, 4D flow MRI has been primarily applied to the whole heart [16–19] and thoracic aorta [20–22]. Less common applications include the evaluation of intracranial [23–25], carotid [26], pulmonary [27, 28] and renal arteries [29, 30]. Gastrointestinal applications are rare and mostly include the evaluation of the hepatic and portal venous flow [31–34].

An exciting new field has emerged in the evaluation and understanding of altered vascular supply of the celiac artery (CA) after esophagectomy and gastric pull-up. This surgical procedure, in combination with radiochemotherapy, is the current gold standard for treatment of esophageal cancer in an operable stage [35–37]. However, this procedure is accompanied by high morbidity and mortality rates of up to 60% and 5%, respectively [38–41], with a major cause of the former being leakage of the anastomosis based on the compromised tissue perfusion of the proximal gastric tube [39, 41, 42]. Several recent publications [43, 44] suggest distinct calcifications of the CA as an independent risk factor for anastomotic leakage after esophagostomy and gastric pull-up. Notably, based on these publications and the clinical routine, a morphological high-grading of stenosis of the CA is not the sole predictor for developing an anastomotic leakage. Vice versa, the absence of a CA stenosis reduces the risk but does not exclude the possibility of an anastomotic leakage. This raises the question of whether there exist flow parameters beyond the sole morphological restrictions of the lumen, and which may be more suitable in predicting outcome and perioperative morbidity of patients with stenosis of the CA. To date, advanced functional flow parameter assessment for the characterization of stenoses in the upper abdomen, particularly in the celiac artery, is lacking. Considering the advantages of this technique, 4D flow MRI has the potential to provide a surrogate parameter to better evaluate and classify vascular stenosis, and ultimately, to enable stratification of patients before surgical procedures such as esophagostomy and gastric pull-up.

Thus, the aim of our study was (1) to examine the feasibility of accelerated 4D flow MRI for the evaluation of stenoses in complex vascular territories in the upper abdomen, and (2) to compare blood flow parameters in the CA and the superior mesenteric artery (SMA) between healthy volunteers and patients with proximal stenosis known from contrast-enhanced computed tomography (CE-CT).

2. Materials and methods

2.1. Study population

This prospective, single-center study was approved by the local ethics committee and was carried out in accordance with the ethical standards as laid down in the Declaration of Helsinki. Written informed consent was obtained from all individual participants (healthy volunteers and patients) included in the study. Exclusion criteria were any contraindications for MRI. The inclusion criteria were: age $>$ 18 years old, absence of any known vascular disease in the group of healthy volunteers, and stenosis at the origin of the CA and/or the SMA confirmed by CE-CT in the patient group. CT imaging was not part of the study protocol. Patients were recruited from the surgical department between 06/2016 and 12/2016. All participants were asked to abstain from eating 4 h prior to the MRI examination in order to minimize artifacts due to peristaltic motion.

2.2. Stenosis evaluation

Stenosis of the CA and the SMA in the patient group was quantified from CT datasets by a radiologist with 4 years of experience in vascular imaging using the AVA (Advanced vessel analysis) tool integrated in IntelliSpace Portal 8.0 (Philips Healthcare, Best, The Netherlands). This commercially available tool allows a semi-automatic evaluation of the grade of stenosis of a vessel according to the NASCET-criteria. In a second step, the velocity-encoded data of the 4D MRI datasets were used to generate a 3D angiography-like luminogram for each healthy volunteer and patient. In this 3D angiography, the severity of the stenosis of the CA and the SMA in patients was manually quantified and compared to the CT datasets. In healthy volunteers, the angiography-like luminogram was assessed to rule out any incidental stenosis of the CA and SMA.

2.3. MRI procedures

All MRI examinations were performed on a clinical, whole-body 3.0 Tesla MR-scanner (Ingenia, Philips Healthcare, Best, The Netherlands), equipped with a standard body-matrix coil and built-in spine matrix coil for signal reception. The position of the healthy volunteers was supine, head-first on the table. The acquired MR protocol consisted of a series of measurements. First, a morphological bTFE (balanced turbo field echo) sequence was acquired in the axial orientation, centered in the upper abdomen. Second, 2D phase contrast (PC)-MRI flow measurements were planned in the para-axial plane perpendicular to the abdominal aorta (AO) proximal to the origin of the CA and paracoronal perpendicular to the CA and SMA. These were followed by the 4D flow measurement where the 3D volume comprised the proximal AO, the CA and the SMA. The bTFE sequence was acquired to obtain an overview of the vasculature in the upper abdomen, and to allow fast and reliable localization of the origin and course of the CA and SMA. The purpose of the 2D PC flow measurement was to approximate the flow velocity in the CA and SMA in order to define the velocity encoding (v_{enc}) value of the 4D flow sequence. The v_{enc} adjustment is crucial, as it must be chosen to be large enough to prevent aliasing artifacts and small enough to assure good velocity-to-noise ratio [15]. As we found flow velocity differences to be distinctive between the AO and the CA and/or SMA, or within the CA and SMA, the 4D flow sequence was mostly acquired twice or threefold with varying v_{enc} settings. In nearly all healthy volunteers, typical v_{enc} values used for measurements were 100 cm/s and 150 cm/s. In patients, typical v_{enc} values were 150 cm/s and 200 cm/s. In five patients, an additional 4D flow sequence was acquired with a v_{enc} value of 250 cm/s, while in two patients, a v_{enc} value of 300 cm/s was necessary to prevent aliasing artifacts along the stenosis. However, higher v_{enc} values led to a reduction of SNR. To achieve a satisfactory temporal resolution, we acquired 24 heart phases per heartbeat for both the 2D as well as the 4D flow sequences. Detailed parameters of all sequences used are given in Table 1. For all flow measurements, a prospective ECG-triggering was used in combination with a *k-t* acceleration factor of 8 and a *k-t* SENSE reconstruction [6, 8]. A pencil-beam navigator placed on the dome of the right diaphragm,

Table 1
Detailed MRI sequence parameters.

		bTFE	2D - PCA	4D - PCA
TR	[ms]	3.0	3.2	4.7
TE	[ms]	1.18	1.83	2.1
Number of slices		28	12	20
Flip angle	[°]	20	10	10
FOV	[mm^2]	350 × 247	350 × 350	200 × 236
Matrix		176 × 114	232 × 224	132 × 128
Slice thickness	[mm]	4	5	1.5
Acq. spatial resolution	[mm^3]	2.0 × 1.6 × 4.0	1.5 × 1.5 × 5.0	1.5 × 1.5 × 1.5
Rec. spatial resolution	[mm^3]	1.0 × 1.0 × 4.0	1.0 × 1.0 × 5.0	0.68 × 0.68 × 1.5
Heart phases		N/A	24	24
Acquisition time	[s]	6	17	150–240[a]
Parallel imaging	(acc. factor)	SENSE (2)	SENSE (2)	*k-t* SENSE (8)
Trigger		no	ECG	ECG, Breathing
Orientation		transversal	para-coronal	3D

PCA = phase contrast angiography; bTFE = Balanced Turbo Field Echo; TR = repetition time; TE = echo time; FOV = field of view; Acq. = Acquired; Rec. = Reconstructed; Heart phases = the number of acquisitions between R-R interval.

[a] Acquisition time without navigator efficiency depending on the v_{enc} setting (higher v_{enc} value ➔ faster acquisition time); the actual scan time of 4D – PCA ranged from 5 to 15 min; N/A – not applicable.

and fixed during the scan, was used to track breathing motion and to gate the 4D flow sequence (acceptance window: 5 mm). Concomitant and eddy-current related phase offsets were corrected by the scanner's reconstruction software.

2.4. Data analysis

Following the MR scan, the acquired data were exported into DICOM format. For data analysis, an established offline 4D flow evaluation tool, GTFlow (GyroTools LCC, Zurich, Switzerland), was employed. This software enables a semi-automatic analysis of flow parameters and was used to measure velocity-related parameters, including peak velocity (PV) and average velocity (AV), as well as flow-related parameters, such as peak flow (PF) and stroke volume (SV). PV (cm/s) depicts the maximal blood flow velocity within the vessel in one pixel, whereas AV (cm/s) describes the maximal blood flow velocity averaged across the whole vessel over an entire cardiac cycle. PF (mL/s) depicts the maximal blood flow volume within the vessel in one pixel, and SV (mL/heartbeat [hb]) represents the blood flow volume passing through the vessel over an entire cardiac cycle.

Mostly, more than one 4D flow sequence was acquired in one session with differing v_{enc} settings. Thus, every acquisition was checked for possible artifacts (e.g. aliasing) or low signal intensity, and each proposed measurement was performed in the acquisition with higher quality (i.e. low artifacts, sufficient velocity-to-noise ratio).

For the measurement of flow parameters, manual segmentation of the vessel wall was performed at the following anatomic landmarks: for the AO, 10 mm proximal to the vessel origin of the CA, between the CA and SMA, and 10 mm distal to the vessel origin of the SMA; in healthy volunteers, 5 mm distal to the vessel ramification of both the CA and SMA, and, in patients, within or, if aggravated, distal to the stenosis.

The blood flow distribution was calculated separately for the CA and SMA as a percentage of the proximal aortic SV. The blood flow distribution into the CA represents the portion of the SV entering the CA from the aortic SV proximal to the outflow of the CA. That into the SMA represents the portion of the SV entering the SMA from the aortic SV in between the outflow of the CA and SMA. To check the quality of the acquired data, we assessed the conservation of mass by comparing the measured SV in the CA and SMA with the SV in the AO (proximal, in between, and distal of the CA and SMA) and calculated the mean error for healthy volunteers and patients separately.

Additionally, average wall shear stress magnitude (N/m^2) was evaluated for the whole vessel as well as for four separate segments of each vessel in a clockwise direction (superior, inferior, left, right). This parameter characterizes the tangential force of the flowing blood on the endothelial surface of the blood vessel and has been linked to various pathological conditions and mechanisms affecting the vascular endothelium [45, 46].

2.5. Statistical analysis

Statistical analyses were performed using SPSS (version 24.0, software IBM, Chicago, IL). Descriptive statistics are given as mean ± standard deviation, if not indicated otherwise. To evaluate the differences in the measured flow parameters between healthy volunteers and patients with known arteriosclerotic stenosis of the CA and SMA close to the vessel origin, two-tailed Student's *t*-tests were performed. Level of significance was assumed if $p \leq 0.05$. Correlations between selected variables were estimated using Pearson's correlation coefficient.

3. Results

3.1. Study population

After establishing the MRI technique, 32 participants were included; 22 of them healthy volunteers (15 m, 7f; mean age: 31.9 ± 12.6 years old; range 23–77 years old) and 10 patients (7 m, 3f; mean age: 74.7 ± 5.3 years old; range 66–82 years old). No incidental stenosis was found in the healthy volunteer group. All patients were referred by the surgical department with esophageal cancer before planned esophagectomy. All patients had a confirmed, proximal stenosis of the CA and/or the SMA diagnosed in oncological staging CT scans within the last 3 months. In total, there were 11 low-grade (CA: 7; SMA: 4) and 5 middle-grade stenoses (CA: 3; SMA: 2) of the CA and SMA ranging from 15.4–33.9% and 50.1–68.2%, respectively. In the following descriptions and discussion, patients with low- or mid-grade stenosis of the CA and/or SMA are not distinguished based on arterial territory – that is, these patients are collectively referred to as *patients with low- or mid-grade stenosis*, respectively. If varying grades of stenosis existed for both, the CA and SMA, the corresponding patient was assigned to the group of the higher stenosis grading (i.e., *patients with mid grade stenosis*). Potential stenoses of other vessels in patients do not fall under this description. Further details are summarized in Table 2.

3.2. Stenosis assessment using velocity encoding data

Pearson's correlation between the degree of stenosis evaluated in contrast-enhanced CT and 4D flow MRI revealed a strong positive correlation for the CA ($r = 0.86$, $p = 0.001$) and to an even greater extent in the SMA ($r = 0.97$, $p = 10e\text{-}6$) (Figs. 1, 2). The absolute differences ranged from 0.5 to 20.6%, with a mean of 7.2 ± 7.1% (CA), and from 0.1 to 11.9% with a mean of 3.5 ± 4.2% (SMA). These differences did not lead to a different grading of the stenosis in any patient. After 4D flow MRI revealed a reliable recognition and evaluation of stenoses in the patients, we used the angiography-like luminogram to examine the healthy volunteers for possible stenoses as these had not undergone CT examinations for this study. No healthy volunteer showed a measurable stenosis of either the CA or SMA.

Table 2
Detailed information about the study population as well as quantification and classification of the stenosis of the CA and SMA in patients according to the NASCET-criteria. Additionally, ROI size and the minimal vessel diameter are presented.

		HV	Patients	
Gender	[m/f]	15/7	7/3	
Mean age ± SD	[y]	31.9 ± 12.6	74.7 ± 5.3	
Age range	[y]	23–77	66–82	
BMI	[kg/m^2]	23.3 ± 2.6	25.1 ± 2.8	
Stenosis grading		N/A	low	middle
Numbers		N/A	11	5
Mean stenosis grade[a] ± SD	[%]	N/A	24.2 ± 6.1	61 ± 6.2
Range	[%]	N/A	15.4–33.9	50.1–68.2
ROI size ± SD	[mm^2]	46.4 ± 17 (CA); 57.6 ± 19.9 (SMA)	20.5 ± 10.4	5.2 ± 1.7
Min. vessel diameter ± SD	[mm]	7.6 ± 1.5 (CA); 8.5 ± 1.4 (SMA)	4.3 ± 1.2	2.5 ± 0.8

BMI = body mass index; m = male; f = female; y = years; HV = Healthy volunteers; SD = standard deviation.
[a] According to NASCET = North American Symptomatic Carotid Endarterectomy Trial, ROI size = area of the minimal residual vessel lumen after manual labeling in the angiography-like luminogram, Min. vessel diameter = minimal diameter of the residual vessel lumen in the angiography-like luminogram; N/A = not applicable.

3.3. Velocity-related parameters

The peak velocity (PV) differed significantly between healthy volunteers and patients with low-grade (105.6 ± 29.9 cm/s vs. 163.5 ± 54.9 cm/s; $p < 0.0001$) and middle-grade stenoses (105.6 ± 29.9 cm/s vs. 192.9 ± 68.7 cm/s; $p < 0.0001$) of the CA/SMA, respectively. Although the PV in patients with middle-grade stenoses was higher than in patients with low-grade stenoses, this difference (Δ = 29.4 cm/s [17.9%]) was not statistically significant ($p = 0.41$).

The average velocity (AV) also differed significantly between healthy volunteers and patients with low-grade (57.1 ± 16.4 cm/s vs. 70.5 ± 22.2 cm/s; $p = 0.03$) and middle-grade stenoses (57.1 ± 16.4 cm/s vs. 90.9 ± 29.8 cm/s; $p < 0.001$) of the CA/SMA. As seen for PV, the AV in patients with middle-grade stenoses was higher than in patients with low-grade stenoses (Δ = 20.4 cm/s [28.9%]) but failed to reach statistical significance ($p = 0.18$). The results are summarized in Table 3 and Fig. 3. An illustration of blood flow velocities in the CA and SMA for a healthy volunteer and a patient with known stenosis of the CA and SMA is given in Fig. 4.

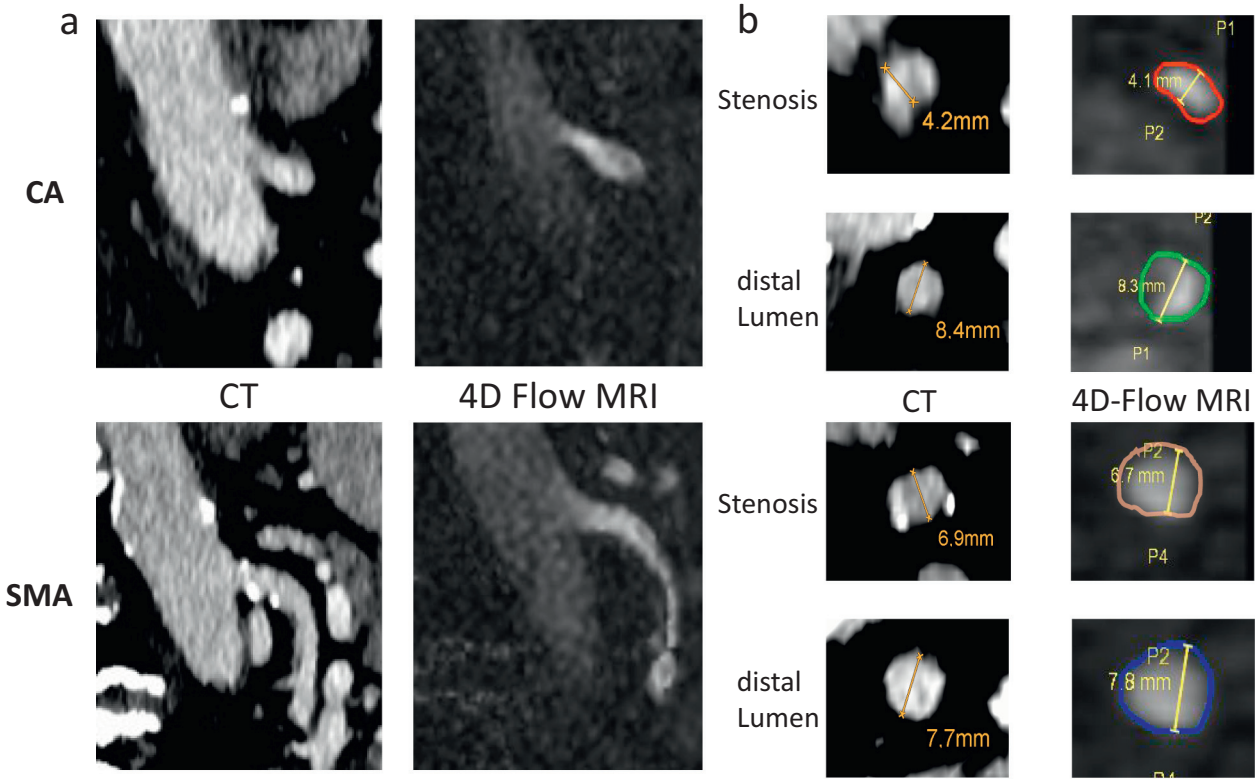

Fig. 1. Comparison of CT-angiography and 4D Flow MRI for stenosis assessment of the CA and SMA in a patient with a mid-grade stenosis of the CA and a low-grade stenosis of the SMA. In the sagittal (a) images, the mid-grade stenosis of the CA can be especially recognized in both CT and 4D flow MRI with additional representation of velocity information (signal intensity) in the angiography-like luminogram. This allowed for an immediate estimate of velocity changes close to the stenosis. In the axial (b) images showing the vessel lumen in an orthograde manner, measurements of the minimal vessel diameter reveal similar results when comparing CT-angiography and 4D flow MRI (see 3.5). The colored marking around the vessel in the MRI images illustrates the associated ROI for flow measurements performed using GTFlow.

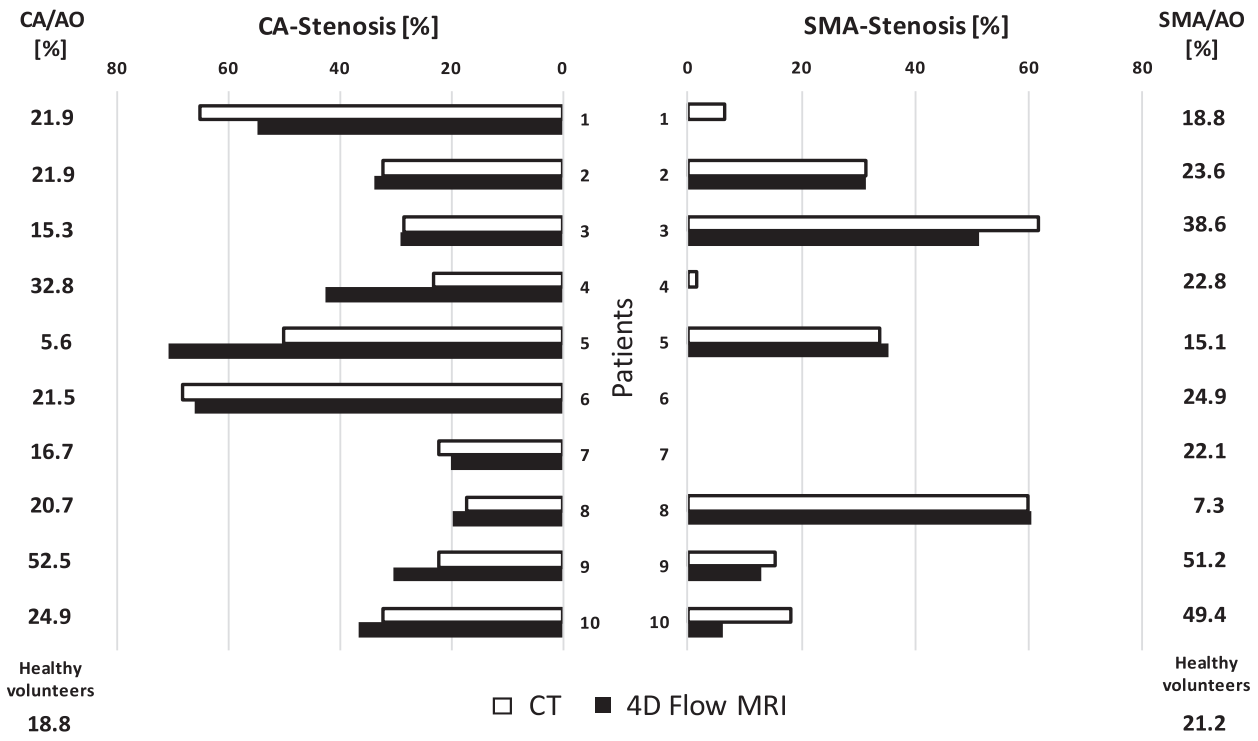

Fig. 2. Degree of stenosis of the CA and SMA for all 10 patients determined in the contrast-enhanced CT and 4D flow datasets using the AVA and GTFlow tools, showing strong (CA, r = 0.86) and very strong (SMA, r = 0.98) correlations. Next to the diagram, relative values of blood flow distribution from the CA (CA/AO) and the SMA (SMA/AO) are given for each patient as well as the mean values of all healthy volunteers.

3.4. Volume-related parameters

The mean peak flow (PF) in the CA and SMA of healthy volunteers was 29 ± 11.9 mL/s. In patients with low-grade stenoses of the CA and SMA, the mean PF was 28.1 ± 9.4 mL/s, while patients with middle-grade stenoses of the CA and SMA had a mean PF of 22.6 ± 12.8 mL/s.

The mean stroke volume (SV) in healthy volunteers was 12 ± 5.3 mL/hb (milliliter per heartbeat) for the CA and SMA. The mean SV in patients with low-grade stenoses of the CA and SMA was 11.5 ± 4.2 mL/hb and in patients with middle-grade stenoses 8.1 ± 4.3 mL/hb.

Both the PF and SV did not differ significantly between healthy volunteers and patients with low- and middle-grade stenoses. However, there was a noticeable trend for higher PF, as well as higher SV, in healthy volunteers and patients with low-grade stenoses relative to patients with middle-grade stenoses (PF: Δ = 22%, p = 0.27 [HV vs. MG]; Δ = 19.6%, p = 0.38 [LG vs. MG]; SV: Δ = 32.5%, p = 0.13 [HV vs. MG]; Δ = 29.6%, p = 0.18 [LG vs. MG]). The results are summarized in Table 3 and Fig. 3. Inter-individual differences in velocity- and flow-related parameters are shown in Fig. 5.

In healthy volunteers, the distribution of the blood volume from the AO during one heartbeat ranged from 6.5 to 32.2% in the CA with a

Table 3
Range, mean values, mean differences (Δ) and p-values for velocity-related parameters (PV, AV), volume-related parameters (PF, SV) and average wall shear stress magnitude (WSS) compared between healthy volunteers (HV) and patients with low (LG)- and middle (MG)-grade stenosis.

		Range	Mean	Mean differences (Δ)			p-Value		
				HV vs. LG	HV vs. MG	LG vs. MG	HV vs. LG	HV vs. MG	LG vs. MG
Velocity related parameter	Peak velocity [cm/s]								
	Healthy volunteers	40.2–181.3	105.6 ± 29.9	57.9 [54.8%]	87.3 [82.7%]	29.4 [17.9%]	< **0.0001**	< **0.0001**	0.41
	Low-grade stenosis	93.2–250.1	163.5 ± 54.9						
	Middle-grade stenosis	89.9–281.8	192.9 ± 68.7						
	Average velocity [cm/s]								
	Healthy volunteers	24.7–95.7	57.1 ± 16.4	13.4 [23.5%]	33.8 [59.2%]	20.4 [28.9%]	**0.03**	< **0.001**	0.18
	Low-grade stenosis	47.9–104.4	70.5 ± 22.2						
	Middle-grade stenosis	52.5–131.3	90.9 ± 29.8						
Volume related parameter	Peak flow [ml/s]								
	Healthy volunteers	5.9–60.9	29 ± 11.9	−0.9 [3.1%]	−6.4 [22%]	−5.5 [19.6%]	0.81	0.27	0.38
	Low-grade stenosis	18.7–44.3	28.1 ± 9.4						
	Middle-grade stenosis	6.8–45.2	22.6 ± 12.8						
	Stroke volume [ml/hb]								
	Healthy volunteers	3.1–31.8	12 ± 5.3	−0.5 [4.2%]	−3.9 [32.5%]	−3.4 [29.6%]	0.79	0.13	0.18
	Low-grade stenosis	5.7–20	11.5 ± 4.2						
	Middle-grade stenosis	2.9–14.4	8.1 ± 4.3						
WSS N/m^2	Healthy volunteers	0.4–1.95	0.92 ± 0.42	0.26 [28.3%]	0.6 [65.2%]	0.34 [28.8%]	0.1	**0.005**	0.29
	Low-grade stenosis	0.5–2.4	1.18 ± 0.57						
	Middle-grade stenosis	0.93–2.04	1.52 ± 0.48						

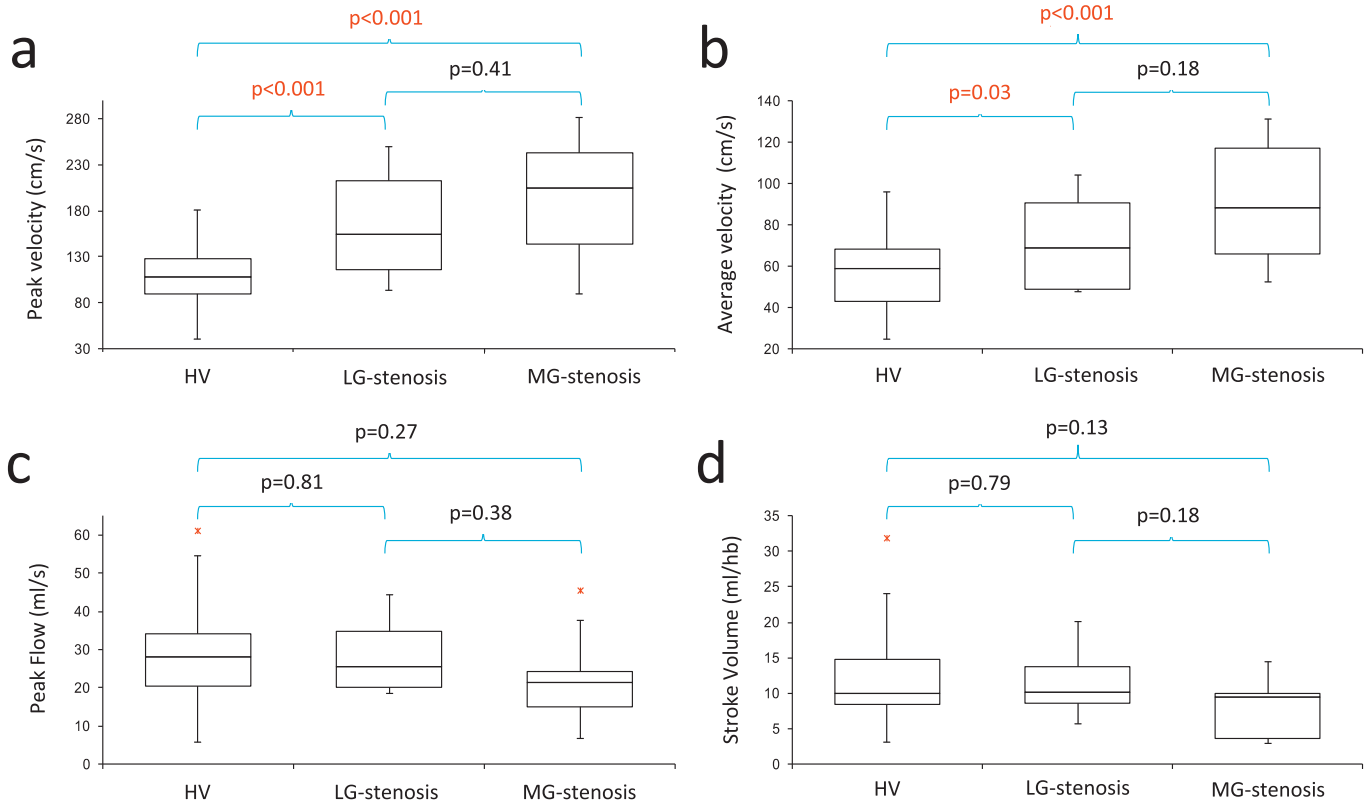

Fig. 3. Box-and-whisker diagrams depicting the values for a. peak velocity (PV), b. average velocity (AV), c. peak flow (PF) and d. stroke volume (SV) for healthy volunteers (HV) and patients with low (LG)- and middle (MG)-grade stenosis. Box plot data represent the five-number summary consisting of: the lowest mean R2* values, the lower quartile (25th percentile), median, upper quartile (75th percentile), and highest mean R2* values. The colored asterisks indicate outliers.

mean of 18.8 ± 6.7% and from 13.8 to 36.5% in the SMA with a mean of 21.2 ± 5.7%. In patients with low-grade stenoses, the distribution of the aortic blood volume ranged from 15.3 to 52.5% in the CA with a mean of 26.4 ± 11.9%, and from 15.1 to 51.2% in the SMA with a mean of 30.9 ± 16.7%. In patients with middle-grade stenoses, values ranged from 5.6 to 21.9% in the CA with a mean of 16.3 ± 7.6%, and from 7.3 to 38.6% in the SMA with a mean of 23 ± 15.6%. These results are summarized in Fig. 2. In patients without any stenosis of the SMA (4 patients), values ranged from 18.8 to 24.9% with a mean of 22.2 ± 2.2%. Pearson's correlation between stenosis grade and distribution of the aortic blood volume was low in the CA ($r = -0.33$,), and appeared to be higher in the SMA ($r = -0.57$,); however, both correlations were not statistically significant ($p = 0.35$; $p = 0.23$).

The assessment of the conservation of mass revealed a mean error of the SV measurements of 7.2% in healthy volunteers and 15.2% in patients.

3.5. Correlation of gender, vessel size (area), BMI, height, weight and flow parameters in healthy volunteers

Male healthy volunteers had a significantly greater vessel size (area) of the CA and SMA than female volunteers (58 ± 18.4 mm^2 vs. 39.3 ± 12.9 mm^2; $p = 0.002$). The vessel size was evaluated by manually marking the vessel wall (ROI). Additionally, the flow volume was significantly higher in men (PF: 33.2 ± 11.3 mL/s; SV: 13.6 ± 5.4 mL/hb vs. PF: 20.2 ± 7.5 mL/s; SV: 8.6 ± 3.3 mL/hb; PF: $p = 0.0004$; SV: $p = 0.004$). In contrast, flow velocities were not significantly influenced by gender. Correlations between BMI and vessel size were modest (CA: $r = 0.24$, $p = 0.28$; SMA: $r = 0.33$, $p = 0.14$) as well as between BMI and flow-related parameters (PF: CA: $r = 0.2$, $p = 0.4$; SMA: $r = 0.29$, $p = 0.2$ / SV: CA: $r = 0.2$, $p = 0.38$; SMA: $r = 0.31$, $p = 0.16$). Strong significant correlations were found between vessel size and flow-related parameters for the CA (PF: CA: $r = 0.72$, $p = 0.0001$; SV: $r = 0.64$, $p = 0.001$) and the SMA (PF: $r = 0.77$, $p = 0.00003$; SV: $r = 0.74$, $p = 0.00008$). Weight [w] and height [h] alone presented low-to-moderate correlations with vessel size of the CA ([w]: $r = 0.32$, $p = 0.14$ /[h]: $r = 0.18$, $p = 0.41$) and the SMA ([w]: $r = 0.65$, $p = 0.001$ /[h]: $r = 0.59$, $p = 0.004$), as well as with the PF of the CA ([w]: $r = 0.47$, $p = 0.03$ /[h]: $r = 0.37$, $p = 0.09$) and the SMA ([w]: $r = 0.6$, $p = 0.003$ /[h]: $r = 0.57$, $p = 0.006$) and the SV of the CA ([w]: $r = 0.56$, $p = 0.007$ /[h]: $r = 0.6$, $p = 0.003$) and the SMA ([w]: $r = 0.62$, $p = 0.002$ /[h]: $r = 0.56$, $p = 0.007$). No correlations were found between BMI, height, weight and velocity-related parameters.

3.6. Wall shear stress

The average WSS magnitude (AWM) in the CA and SMA ranged from 0.34 to 1.95 N/m^2 in healthy individuals, from 0.62 to 2.42 N/m^2 in patients with low-grade stenoses and from 0.93 to 1.9 N/mm^2 in patients with middle-grade stenoses. Patients with middle-grade stenoses had a significantly higher AWM than healthy individuals (HV: 0.96 ± 0.44 N/m^2 vs. MG: 1.56 ± 0.34 N/m^2; $p = 0.02$). Although AWM was higher in patients with low-grade stenoses (LG: 1.26 ± 0.52 N/m^2) compared to healthy individuals ($\Delta = 0.3$ N/m^2 [31.3%]), this difference did not reach statistical significance ($p = 0.06$).

For a more thorough analysis of WSS, we divided the lumen of the vessel into 4 segments equivalent to quadrants of equal area (1 = superior, 2 = left, 3 = inferior, 4 = right) and evaluated AWM within each of these segments in both the CA and SMA. Patients with low-grade stenoses revealed a significantly higher AWM in segments 1, 2 and 4 ($p = 0.0008/0.009/0.004$) compared to healthy volunteers. Patients with middle-grade stenoses had a significantly higher AWM in

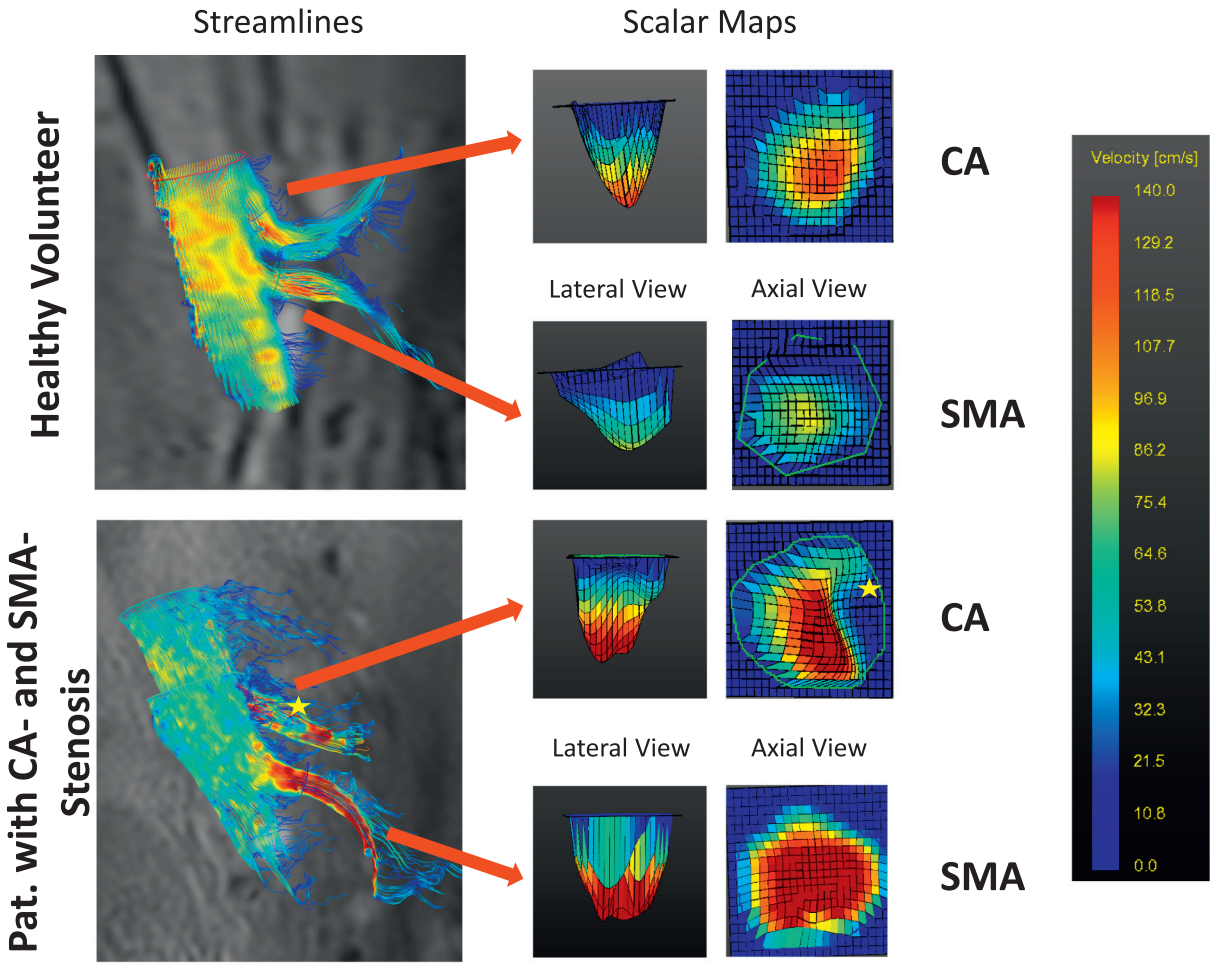

Fig. 4. Illustration of flow pattern during systole using time-resolved 3D-streamlines which allow visualization of velocity changes in a HV (top panel) as well as a patient with known stenosis of the CA and SMA (bottom panel). Scalar maps show the distribution of blood flow velocity in the vessel lumen of the CA and SMA. Note: the yellow star represents a local turbulence with reduced blood flow velocity. (For interpretation of the references to color in this figure legend, the reader is referred to the web version of this article.)

all 4 segments (p = 2.2e-6/2e-7/0.03/0.004) compared to healthy volunteers. Patients with middle-grade stenoses had a significantly higher AWM in segment 2 (p = 0.02) compared to patients with low-grade stenoses. The results are summarized in Fig. 6.

4. Discussion

This study explored the feasibility of 4D flow MRI for the assessment of proximal stenosis of the CA and SMA in patients as well as in healthy volunteers. Patients with stenosis revealed a significantly altered flow profile, compared to healthy volunteers, in the form of increased velocity-related parameters. Accordingly, CA or SMA stenosis tended to result in decreased volume-related parameters depending on the stenosis grade.

At present, changes in 4D flow MRI parameters due to stenosis were only described in a limited number of patients with intracranial stenosis [23, 24] and in peripheral territories such as the iliac or femoral arteries [47]. Both Hope et al. [23] and Frydrychowicz et al. [47] showed increased flow velocity in all 3 patients with known stenosis. The quantification of peak velocities along the moderate stenosis of the common and external iliac arteries was reported to be twice as high than for the rest of the vessels (65 cm/s vs. 32 cm/s) [47]. In intracranial stenosis [23], the velocity parameters were moderately higher in a minor stenosis of the middle cerebral artery (PV: Δ ≈ 30%) and significantly higher in a middle-grade stenosis (PV: 76 vs 43 cm/s; Δ = 77%) when compared to the contralateral side. Wu et al. [24] presented data from intracranial vessels in healthy volunteers and patients with unilateral stenosis of the internal carotid artery or middle cerebral artery. All 10 healthy volunteers showed similar and coherent blood flow velocities and patterns when comparing the left and right cerebral arteries, whereas the 22 patients revealed a compromised blood flow on the side of the stenosis compared to the contralateral side. Notably, these results are only given as semi-quantitative comparisons and not as absolute flow data. The authors conclude that 4D flow MRI can provide additional hemodynamic information, as regional atherosclerotic lesions can not only alter local vascular flow dynamics but also influence hemodynamics in other vascular territories.

For both flow- and volume-related parameters, a relatively large inter-individual range was found not only for the patients with stenosis but also for healthy volunteers. Most flow parameters reach statistical significance depending on the stenosis grade; however, there was a broad overlap between the different groups (i.e. healthy volunteers vs. stenosis grades). This suggests that these groups differed in terms of the morphologic grade of CA and SMA stenoses, but the flow volume seems to be heterogeneously sustained. Consequently, morphologic evaluation alone does not seem to sufficiently estimate possible vascular dysfunction due to stenosis. Extrapolating these findings to the clinical scenario of anastomotic leakage after gastric pull-up, this might partly explain the varying outcome observed in patients with CA stenoses. Rather, it is plausible that 4D flow MRI may help to better differentiate

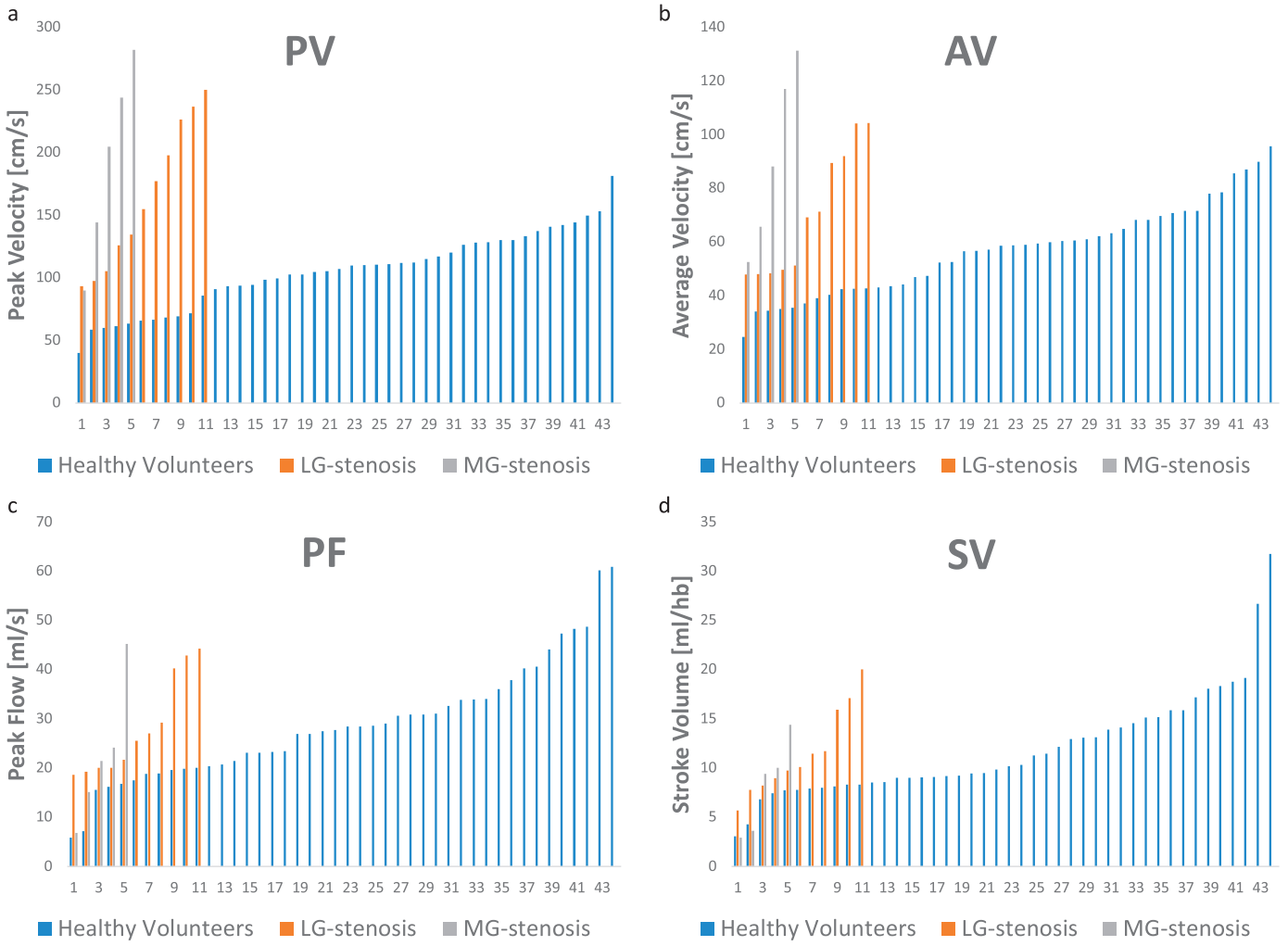

Fig. 5. Waterfall plots showing the values for a. peak velocity (PV), b. average velocity (AV), c. peak flow (PF) and d. stroke volume (SV) for all 22 healthy volunteers (HV) (44 vessels) and 10 patients with low (LG)- and middle (MG)-grade stenosis (16 stenoses). Note: the values are given in ascending order and combine both CA and SMA.

patients with similar morphology but distinct flow parameters of stenosis. In this context, the relative distribution of the blood volume of the AO can be an interesting parameter, which was found to be heterogeneous among healthy volunteers as well as in patients with stenosis. The grade of the stenosis alone does not seem to be a sufficient reason for this variability, as the correlation between stenosis grade and relative volume was modest, particularly in the CA, and not statistically significant. However, from our point of view, the results do not allow for a prognosis of the surgical outcome. Also, gender differences in our results and their effect on the surgical outcome are difficult to analyze as > 80% of patients are men [48, 49].

These data are in line with publications confirming substantial inter-individual differences in flow velocity and flow volume in the CA and SMA. For example, Wiedemann [50] employed Doppler-sonography to evaluate flow parameters of vessels in the upper abdomen. The author found that flow velocity ranged from 47.9 to 310 cm/s (mean: 108.8 cm/s) in the CA and 72.7 to 211.7 cm/s (mean: 112 cm/s) in the SMA; furthermore, flow volume ranged from 8.5 to 25.7 mL/s (mean: 10.2 mL/s) in the CA and from 5.8 to 14.8 mL/s (mean: 8.7 mL) in the SMA. Byrne et al. [51] compared flow parameters between controls and patients with Crohn's disease using Doppler-sonography finding a similar mean AV (44 cm/s) and mean SV (15.4 mL/s) in controls compared to the current study.

Currently, the literature lacks sufficiently reliable and comparable data of 4D flow MRI of abdominal stenoses. Nevertheless, Stankovic and coworkers [31] examined 16 healthy volunteers at 3 T with the aim of evaluating liver hemodynamics and the influence of various acceleration factors using a *k-t* GRAPPA accelerated 3D-sequence. Peak and average velocities, as well as flow volume, were measured in the CA and SMA of healthy volunteers. Yet, the reported mean values for peak/average velocity were found to be lower (PV: $\Delta = 30$ mL/s; AV: $\Delta = 25$ mL/s) than the values of the current study, although values for flow volume did not differ substantially. The authors did not show ranges of the flow parameters, but the standard deviations strongly indicate a definite variation in the CA, thus supporting our results. Dyvorne et al. [52] who evaluated different 4D flow MRI acquisition techniques found a lower time-averaged total flow (CA: 7.3 mL/s; SMA: 5.6 mL/s) compared to SV measured in the current study. AV for CA and SMA did not differ substantially. However, this comparison is limited as Dyvorne et al. included healthy volunteers as well as patients with liver disease. Technical reasons for the differences in the absolute values due to different MRI manufacturers or diverging sequences should be considered rather circumstantial.

Other potential factors such as BMI, age and gender did not influence the flow velocity of the CA and SMA. However, vessel size (area) correlated positively with the flow volume of the CA and SMA—an observation unique to men given their systematically greater vessel size (area) [53]. Recent 4D flow MRI studies did not assess these aspects in

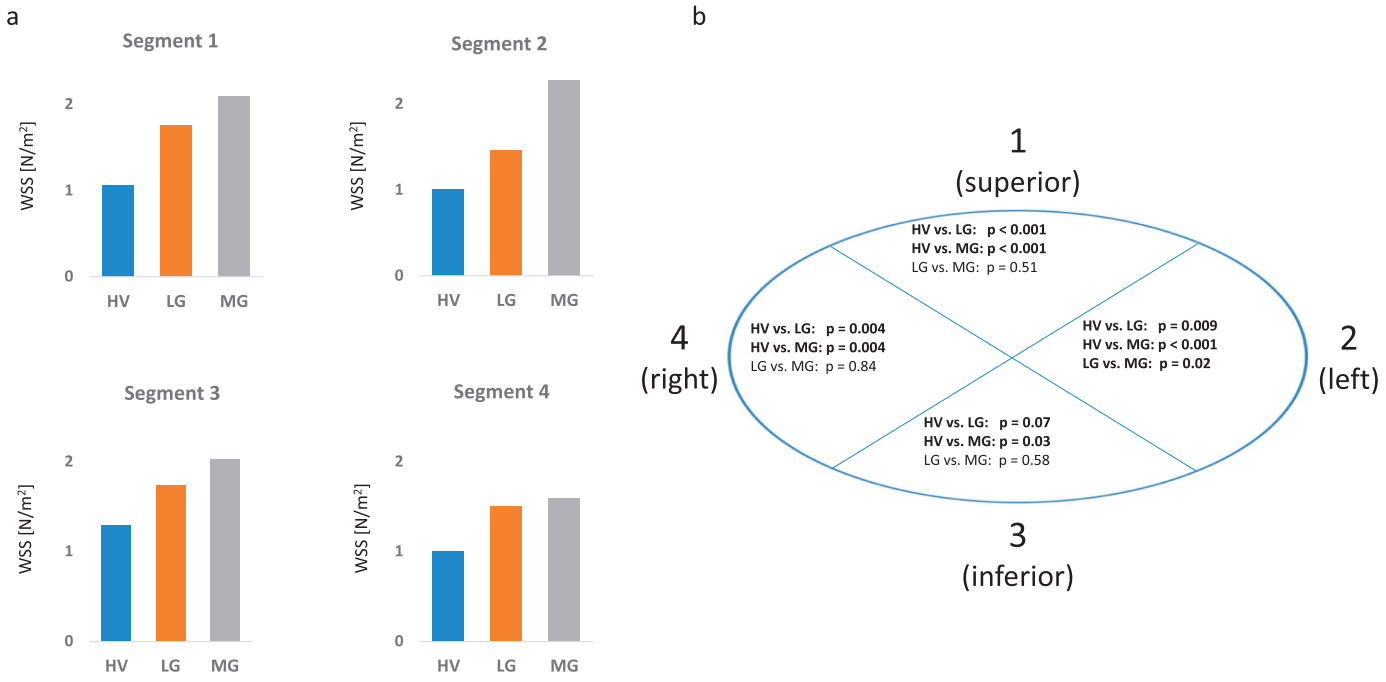

Fig. 6. Average WSS magnitude (N/m^2) for healthy volunteers (HV) and patients with low (LG)- and middle (MG)-grade stenosis of the CA and SMA for each segment. A: Comparison of mean values of average WSS magnitude for each group and segment. B: Cross-section of the CA or SMA illustrating the segmentation and p-values for each comparison of average WSS magnitude per group and segment.

their subject groups.

Further, additional 4D flow MRI parameters, such as wall shear stress, also revealed significant differences between healthy volunteers and patients. Our results are in line with ex vivo model-based studies [54] and in vivo studies dealing with carotid arteries [55] showing increased wall shear stress with increasing grade of stenosis. For the in-vivo study, an interesting aspect is that the magnitude of WSS is much greater in carotid arteries with stenoses than in healthy carotid arteries. Additionally, WSS varied for parts of the vessel in the stenotic region (internal side of bifurcation of carotid artery) comparable to the differences we detected for the 4 segments of the vessel.

Such parameters may be of interest in future studies, especially in the post-surgical setting where complex changes in the orientation of the CA occur after gastric pull-up.

Besides the dedicated 4D flow parameters, the 3D velocity encoding data can be used to generate an angiography-like luminogram. Given the lack of the gold standard CT examination, we assessed these datasets to exclude any incidental stenosis of the CA and SMA in the participating healthy individuals. Conversely, the degree of stenosis of the CA and SMA determined by CE-CT and 3D velocity encoding data was compared, revealing strong correlations in both the CA and SMA, with a mean difference of < 10%. This suggests that 4D flow MRI seems to be reliable for evaluation of the severity of a vessel stenosis, further indicating that a prior contrast-enhanced CT may not be necessary for vessel stenosis grading.

In our study, a few limitations should be discussed: (1) The number of patients with mid-grade stenoses of the CA and/or SMA was limited, probably resulting in non-significant differences between low- and mid-grade stenoses for flow velocity and flow volume. (2) Within the recruitment period, no patients were included in the study with a high-grade stenosis of the CA or the SMA. Consequently, further investigation should evaluate flow parameters in this patient group, where a substantial increase in flow velocity and decrease in flow volume would be expected in some patients. (3) Duplex-ultrasound was not included in our study protocol for verification of blood flow speed as we believe that the relative comparison of blood flow parameters between healthy volunteers and patients, as a function of stenosis, is most relevant in this study, especially for blood flow velocity. Such differences are likely more relevant for vessel analysis than the absolute values gained from duplex-ultrasound alone. Furthermore, and to the best of our knowledge, a validation of 4D flow MRI in gastrointestinal vessels, especially with associated stenoses, has not been previously published; therefore, we would not be able to confirm the accuracy of the blood flow parameters measured by duplex-ultrasound. (4) A high spatio-temporal acceleration factor was used in our study, in order to achieve satisfactory spatial and temporal resolutions with acquisition times still acceptable for our patients. A *k-t* SENSE reconstruction provided by the manufacturer was used. The potential temporal blurring effect, known to affect velocity curves at high acceleration factors in combination with *k-t* SENSE has not been assessed, as no gold standard data were available. Further investigation should evaluate advanced reconstruction techniques (*k-t* PCA) known to minimize temporal blurring [8, 56]. (5) The large velocity spectrum measured in patients and volunteers further confirms the need for a 4D flow sequence that simultaneously measures slow and fast velocities. This multi-v_{enc} technique would further avoid the often cumbersome and time-intensive assessment of the optimal v_{enc} value.

5. Conclusions

In conclusion, our study shows that 4D flow MRI is a technique feasible for the evaluation of complex flow characteristics in smaller vessels such as the celiac trunk and the superior mesenteric artery. This technique provides functional information beyond the pure morphology as obtained in contrast-enhanced CT. Studies concerning validation of 4D flow MRI in small vessels are needed before future clinical implementation. A highly promising prospect could be the preoperative evaluation before esophagostomy to better differentiate patients without functional constraints from patients with relevant restriction of blood flow through the supplying artery (celiac trunk), despite both patient groups showing similar morphology of stenoses.

Funding

This research did not receive any specific grant from funding agencies in the public, commercial, or not-for-profit sectors.

Declarations of interest

Kilian Weiss is an employee of Philips Healthcare Germany. All other authors have no conflict of interest.

Informed consent

Informed consent was obtained from all individual participants included in the study after the nature of the procedure had been fully explained.

References

[1] Bonow RO, Carabello BA, Chatterjee K, de Leon Jr. AC, Faxon DP, Freed MD, et al. ACC/AHA 2006 guidelines for the management of patients with valvular heart disease. J Am Coll Cardiol 2006;48:1–148.
[2] Firmin DN, Gatehouse PD, Konrad JP, Yang GZ, Kilner PJ, Longmore DB. Rapid 7-dimensional imaging of pulsatile flow. Comput IEEE Comput Soc 1993;14:353–6.
[3] Wigström L, Sjöqvist L, Wranne B. Temporally resolved 3D phase-contrast imaging. Magn Reson Med 1996;36:800–3.
[4] Pruessmann KP, Weiger M, Scheidegger MB, Boesiger P. SENSE: sensitivity encoding for fast MRI. Magn Reson Med 1999;42:952–62.
[5] Griswold MA, Blaimer M, Breuer F, Heidemann RM, Mueller M, Jakob PM. Parallel magnetic resonance imaging using the GRAPPA operator formalism. Magn Reson Med 2005;54:1553–6.
[6] Tsao J, Boesiger P, Pruessmann K. k-t BLAST and k-t SENSE: dynamic MRI with high frame rate exploiting spatiotemporal correlations. Magn Reson Med 2003;50:1031–42.
[7] Baltes C, Kozerke S, Hansen MS, Pruessmann KP, Tsao J, Boesiger P. Accelerating cine phase-contrast flow measurements using k-t BLAST and k-t SENSE. Magn Reson Med 2005;54:1430–8.
[8] Giese D, Wong J, Greil GF, Buehrer M, Schaeffter T, Kozerke S. Towards highly accelerated Cartesian time-resolved 3D flow cardiovascular magnetic resonance in the clinical setting. J Cardiovasc Magn Reson 2014;16:42.
[9] Dyverfeldt P, Bissell M, Barker AJ, Bolger AF, Carlhäll CJ, Ebbers T, et al. 4D flow cardiovascular magnetic resonance consensus statement. J Cardiovasc Magn Reson 2015;17:72.
[10] Wigström L, Ebbers T, Fyrenius A, Karlsson M, Engvall J, Wranne B, et al. Particle trace visualization of intracardiac flow using time-resolved 3D phase contrast MRI. Magn Reson Med 1999;41:793–9.
[11] Kozerke S, Hasenkam JM, Pedersen EM, Boesiger P. Visualization of flow patterns distal to aortic valve prostheses in humans using a fast approach for cine 3D velocity mapping. J Magn Reson Imaging 2001;13:690–8.
[12] Fyrenius A, Wigström L, Ebber T, Karlsson M, Engvall J, Bolger AF. Three dimensional flow in the human left atrium. Heart 2001;86:448–55.
[13] Bürk J, Blanke P, Stankovic Z, Barker A, Russe M, Geiger J, et al. Evaluation of 3D blood flow patterns and wall shear stress in the normal and dilated thoracic aorta using flow-sensitive 4D CMR. J Cardiovasc Magn Reson 2012;14:84.
[14] Frydrychowicz A, Franc CJ, Turski PA. Four-dimensional phase contrast magnetic resonance angiography: potential clinical applications. Eur J Radiol 2011;80:24–35.
[15] Stankovic Z, Allen BD, Garcia J, Jarvis KB, Markl M. 4D flow imaging with MRI. Cardiovasc Diagn Ther 2014;4:173–92.
[16] Kilner PJ, Yang GZ, Wilkes AJ, Mohiaddin RH, Firmin DN, Yacoub MH. Asymmetric redirection of flow through the heart. Nature 2000;404:759–61.
[17] Bolger AF, Heiberg E, Karlsson M, Wigström L, Engvall J, Sigfridsson A, et al. Transit of blood flow through the human left ventricle mapped by cardiovascular magnetic resonance. J Cardiovasc Magn Reson 2007;9:741–7.
[18] Geiger J, Markl M, Jung B, Grohmann J, Stiller B, Langer M, et al. 4D-MR flow analysis in patients after repair for tetralogy of Fallot. Eur Radiol 2011;21:1651–7.
[19] François CJ, Srinivasan S, Schiebler ML, Reeder SB, Niespodzany E, Landgraf BR, et al. 4D cardiovascular magnetic resonance velocity mapping of alterations of right heart flow patterns and main pulmonary artery hemodynamics in tetralogy of Fallot. J Cardiovasc Magn Reson 2012;14:16.
[20] Bogren HG, Buonocore MH, Valente RJ. Four-dimensional magnetic resonance velocity mapping of blood flow patterns in the aorta in patients with atherosclerotic coronary artery disease compared to age-matched normal subjects. J Magn Reson Imaging 2004;19:417–27.
[21] Kvitting JP, Ebbers T, Wigström L, Engvall J, Olin CL, Bolger AF. Flow patterns in the aortic root and the aorta studied with time-resolved, 3-dimensional, phase-contrast magnetic resonance imaging: implications for aortic valce-sparing surgery. J Thorac Cardiovasc Surg 2004;127:1602–7.
[22] Markl M, Draney MT, Miller DC, Levin JM, Williamson EE, Pelc NJ, et al. J Thorac Cardiovasc Surg 2005;130:456–63.
[23] Hope TA, Hope MD, Purcell DD, von Morze C, Vigneron DB, Alley MT, et al. Evaluation of intracranial stenoses and aneurysms with accelerated 4D flow. Magn Reson Imaging 2010;28:41–6.
[24] Wu C, Schnell S, Vakil P, Honarmand AR, Ansari SA, Carr J, et al. In vivo assessment of the impact of regional intracranial atherosclerotic lesions on brain arterial 3D hemodynamics. Am J Neuroradiol 2017;38:515–22.
[25] Ansari SA, Schnell S, Carroll T, Vakil P, Hurley MC, Wu C, et al. Intracranial 4D flow MRI: toward individualized assessment of arteriovenous malformation hemodynamics and treatment-induced changes. AJNR Am J Neuroradiol 2013;34:1922–8.
[26] Harloff A, Zech T, Wegent F, Strecker C, Weiller C, Markl M. Comparison of blood flow velocity quantification by 4D flow MR imaging with ultrasound at the carotid bifurcation. AJNR Am J Neuroradiol 2014;34:1407–13.
[27] Tariq U, Hsiao A, Alley M, Zhang T, Lustig M, Vasanawala SS. Venous and arterial flow quantification are equally accurate and precise with parallel imaging compressed sensing 4D phase contrast MRI. J Magn Reson Imaging 2013;37:1419–26.
[28] Bächler P, Pinochet N, Sotelo J, Crelier G, Irarrazaval P, Tejos C, et al. Assessment of normal flow patterns in the pulmonary circulation by using 4D magnetic resonance velocity mapping. Magn Reson Imaging 2013;31:178–88.
[29] François CJ, Lum DP, Johnson KM, Landgraf KM, Bley TA, Reeder SB, et al. Renal arteries: isotropic, high-spatial-resolution, unenhanced MR angiography with three-dimensional radial phase contrast. Radiology 2011;258:254–60.
[30] Bley TA, Johnson KM, Francois CJ, Reeder SB, Schiebler ML, Landgraf BR, et al. Noninvasive assessment of transstenotic pressure gradients in porcine renal artery stenoses by using vastly undersampled phase-contrast MR angiography. Radiology 2011;261:266–73.
[31] Stankovic Z, Fink J, Collins JD, Sermaan E, Russe MF, Carr JC, et al. K-t GRAPPA-accelerated 4D flow MRI of liver hemodynamics: influence of different acceleration factors on qualitative and quantitative assessment of blood flow. MAGMA 2015;28:149–59.
[32] Stankovic Z, Csatari Z, Deibert P, Euringer W, Jung B, Kreisel W, et al. A feasibility study to evaluate splanchnic arterial and venous hemodynamics by flow-sensitive 4D MRI compared with Doppler ultrasound in patients with cirrhosis and controls. Eur J Gastroenterol Hepatol 2013;25:669–75.
[33] Frydrychowicz A, Landgraf BR, Niespodzany E, Verma RW, Roldán-Alzate A, Johnson KM, et al. Four-dimensional velocity mapping of the hepatic and splanchnic vasculature with radial sampling at 3 tesla: a feasibility study in portal hypertension. J Magn Reson Imaging 2011;34:577–84.
[34] Roldán-Alzate A, Frydrychowicz A, Niespodzany E, Landgraf BR, Johnson KM, Wieben O, et al. In vivo validation of 4D flow MRI for assessing the hemodynamics of portal hypertension. J Magn Reson Imaging 2013;37:1100–8.
[35] van Hagen P, Hulshof MC, van Lanschot JJ, Steyerberg EW, van Berge Henegouwen MI, Wijnhoven BP, et al. Preoperative chemoradiotherapy for esophageal or junctional cancer. N Engl J Med 2012;366:2074–84.
[36] Kumagai K, Rouvelas I, Tsai JA, Mariosa D, Lind PA, Lindblad M, et al. Survival benefit and additional value of preoperative chemoradiotherapy in resectable gastric and gastro-oesophageal junction cancer: a direct and adjusted indirect comparison meta-analysis. Eur J Surg Oncol 2015;41:282–94.
[37] D'Journo XB, Thomas PA. Current management of esophageal cancer. J Thorac Dis 2014;6:253–64.
[38] Alldinger I, Sisic L, Hochreiter M, Weichert W, Blank S, Burian M, et al. Outcome, complications, and mortality of an intrathoracic anastomosis in esophageal cancer in patients without a preoperative selection with a risk score. Langenbecks Arch Surg 2015;400:9–18.
[39] Paul S, Altorki N. Outcomes in the management of esophageal cancer. J Surg Oncol 2014;110:599–610.
[40] Rutegård M, Lagergren P, Rouvelas I, Lagergren J. Intrathoracic anastomotic leakage and mortality after esophageal cancer resection: a population-based study. Ann Surg Oncol 2012;19:99–103.
[41] Briel JW, Tamhankar AP, Hagen JA, DeMeester SR, Johansson J, Choustoulakis E, et al. Prevalence and risk factors for ischemia, leak, and stricture of esophageal anastomosis: gastric pull-up versus colon interposition. J Am Coll Surg 2004;198:536–41.
[42] Zehetner J, DeMeester SR, Alicuben ET, Oh DS, Lipham JC, Hagen JA, et al. Intraoperative assessment of perfusion of the gastric graft and correlation with anastomotic leaks after esophagectomy. Ann Surg 2014;262:74–8.
[43] van Rossum PSN, Haverkamp L, Verkooijen HM, van Leeuwen MS, van Hillegersberg R, Ruurda JP. Calcification of arteries supplying the gastric tube: a new risk factor for anastomotic leakage after esophageal surgery. Radiology 2015;274:124–32.
[44] Zhao L, Zhao G, Li J, Qu B, Shi S, Feng X, et al. Calcification of arteries supplying the gastric tube increases the risk of anastomotic leakage after esophagectomy with cervical anastomosis. J Thorac Dis 2016;8:3551–62.
[45] Oshinski JN, Ku DN, Mukundan S, Loth F, Pettigrew RI. Determination of wall shear stress in the aorta with the use of MR phase velocity mapping. J Magn Reson Imaging 1995;5:640–7.
[46] Davies PF, Mundel T, Barbee KA. A mechanism for heterogeneous endothelial responses to flow in vivo and in vitro. J Biomech 1995;28:1553–60.
[47] Frydrychowicz A, Winterer JT, Zaitsev M, Jung B, Hennig J, Langer M, et al. Visualization of iliac and proximal femoral artery hemodynamics using time-resolved 3D phase contrast MRI at 3T. J Magn Reson Imaging 2007;25:1085–92.
[48] Glatz T, Marjanovic G, Kulemann B, Sick O, Hopt UT, Hoeppner. Hybrid minimally invasive esophagectomy vs. open esophagectomy: a matched case analysis in 120 patients. Langenbecks Arch Surg 2017;402:323–31.
[49] Luan A, Hunter CL, Crowe CS, Lee GK. Comparison of outcomes of total esophageal reconstruction with supercharged jejunal flap, colonic interposition, and gastric pull-up. Ann Plast Surg 2018;80:S274–8.
[50] Wiedemann H. Dopplersonographische Untersuchung der Leberperfusion in Ruhe und Berücksichtigung der Regulation unter Belastung und postprandial – eine

experimentelle Studie zur Normwerterhebung. Hamburg. 2000.
[51] Byrne MF, Farrell MA, Abass S, Fitzgerald A, Varghese JC, Thornton F, et al. Assessment of Crohn's disease activity by Doppler sonography of the superior mesenteric artery, clinical evaluation and the Crohn's disease activity index: a prospective study. Clin Radiol 2001;56:973–8.
[52] Dyvorne H, Knight-Greenfield A, Jajamovich G, Besa C, Cui Y, Stalder A, et al. Abdominal 4D flow MR imaging in a breath hold: combination of spiral sampling and dynamic compressed sensing for highly accelerated acquisition. Radiology 2015;275:245–54.
[53] Huxley VH. Sex and the cardiovascular system: the intriguing tale of how women and men regulate cardiovascular function differently. Adv Physiol Educ 2007;31:17–22.
[54] Zhou Y, Lee C, Wang J. The computational fluid dynamics analyses on hemodynamic characteristics in stenosed arterial models. J Healthc Eng 2018;2018:4312415.
[55] Bit A, Ghagare D, Rizvanov AA, Chattopadhyay. Assessment of influences of stenoses in right carotid artery on left carotid artery using wall stress marker. Biomed Res Int 2017;2017:2935195.
[56] Pedersen H, Kozerke S, Ringgaard S, Nehrke K, Won YK. K-t PCA: temporally constrained k-t BLAST reconstruction using principal component analysis. Magn Reson Med 2009;62:706–16.